PALEOCEANOGRAPHY, VOL. 28, 116–129, doi:10.1002/palo.20020, 2013

The dynamics of the marine nitrogen cycle across the last deglaciation

Olivier Eugster,[1] Nicolas Gruber,[1] Curtis Deutsch,[2] Samuel L. Jaccard,[3] and Mark R. Payne[1,4]

Received 10 August 2012; revised 12 February 2013; accepted 14 February 2013; published 23 March 2013.

[1] We use a geochemical box model to investigate the changes in marine N-fixation and denitrification required to match the observed sedimentary $\delta^{15}N$ changes between ~30 kyr B.P. and the late Holocene. This is achieved by optimizing a set of seven parameters that describe the strengths of three ocean-internal N feedbacks and the response of the oceanic N cycle to four external forcings. Scenarios that best match the $\delta^{15}N$ constraints indicate a strong transient decrease in N-fixation in the early deglacial in response to the decrease in iron input by dust. Around 15 kyr B.P., N-fixation rebounds primarily in response to an abrupt increase in water column denitrification caused by an expansion of anoxia. Benthic denitrification is not well constrained by our model but tends to increase in sync with water column denitrification. As a result of the transient imbalance between N-fixation and denitrification, we infer a glacial-to-interglacial decrease in the marine N inventory of between 15 and 50%. The model diagnoses this reduction in order to simultaneously fit the data from all ocean basins, requiring it to reduce the degree by which water column denitrification in the oxygen minimum zones is influencing the $\delta^{15}N$ of nitrate of the whole ocean (dilution effect). Our optimal solution suggests a glacial N cycle that operated at nearly the same rates as that in pre-industrial times, but sensitivity cases with substantially lower rates fit the data only marginally worse. An important caveat of our study is the assumption of an unchanging ocean circulation. An initial sensitivity experiment shows that this affects primarily the magnitude of the change in the N inventory, while the diagnosed deglacial dynamics with global marine N-fixation taking a dip before the onset of denitrification remains a robust result.

Citation: Eugster, O., N. Gruber, C. Deutsch, S. L. Jaccard, and M. R. Payne (2013), The dynamics of the marine nitrogen cycle across the last deglaciation, *Paleoceanography*, *28*, 116–129, doi:10.1002/palo.20020.

1. Introduction

[2] A higher glacial inventory of fixed N in the ocean has been proposed as one of the many hypotheses to explain the enigmatic change in atmospheric CO_2 across the glacial-interglacial transitions [*McElroy*, 1983; *Falkowski*, 1997; *Broecker and Henderson*, 1998; *Archer et al.*, 2000]. Given that fixed N, i.e., all forms of nitrogen with the exception of molecular nitrogen, is considered as the most important limiting nutrient in the ocean for phytoplankton growth, such a higher inventory would have allowed greater biological sequestration of atmospheric CO_2 in the ocean interior (see Figure 1). A larger glacial inventory of N could have been created by a transient imbalance between the dominant source and sink of N, i.e., N-fixation and denitrification [*Capone et al.*, 1997; *Codispoti et al.*, 2001], respectively, across the deglaciation. But changes in sources and sinks are not well established, and, as a consequence, the extent to which the inventory of N varied across the transition remains elusive [*Gruber*, 2004].

[3] Among the most useful tools to assess glacial-interglacial changes in the marine N cycle is the stable isotopic ratio, $^{15}N/^{14}N$ (expressed as $\delta^{15}N = (^{15}N/^{14}N)_{sample}/(^{15}N/^{14}N)_{ref} - 1$, the universal reference is N_2 in air) of organic N preserved in marine sediments [e.g., *Altabet et al.*, 1991, 1995; *Francois et al.*, 1992; *Haug et al.*, 1998; *Kienast*, 2000; *Deutsch et al.*, 2004; *Ren et al.*, 2009; *Meckler et al.*, 2011]. The usefulness of this proxy is based on the distinct isotopic fractionations associated with N-fixation, denitrification in the water column and in benthic environments, and N assimilation by phytoplankton [*Cline and Kaplan*, 1975].

All Supporting Information may be found in the online version of this article.

[1]Environmental Physics, Institute of Biogeochemistry and Pollutant Dynamics, ETH Zurich, Zurich, Switzerland.
[2]Department of Atmospheric and Oceanic Sciences, University of California, Los Angeles, California, USA.
[3]Geological Institute, ETH Zurich, Zurich, Switzerland.
[4]National Institute of Aquatic Resources (DTU-Aqua), Technical University of Denmark, Charlottenlund, Denmark.

Corresponding author: O. Eugster, Environmental Physics, Institute of Biogeochemistry and Pollutant Dynamics, ETH Zürich, CHN E27, Universitätstr. 16, 8092 Zürich, Switzerland. (olivier.eugster@env.ethz.ch)

0883-8305/13/10.1002/palo.20020

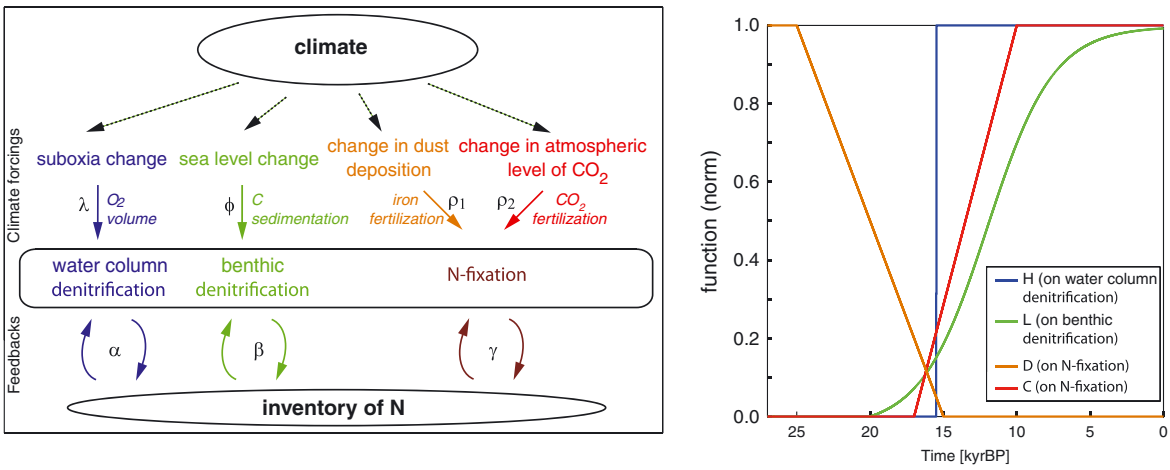

Figure 1. Forcings and feedbacks in the model. (Left panel) Sketch of the simulated climate forcings and internal feedbacks of the marine N cycle. (Right panel) Timing of the four climate forcings. $H(t)$.

[4] The strongest $\delta^{15}N$ signals across the last deglaciation are found in records from the oxygen minimum zones (OMZ), such as the Arabian Sea and the Eastern Tropical North and South Pacific, where water column denitrification is dominating the local $\delta^{15}N$ of NO_3^- [*Brandes et al.*, 1998]. These records reveal a sharp increase in $\delta^{15}N$ of up to 6‰ between the Last Glacial Maximum (LGM) and the early Holocene followed by a decrease of smaller amplitude towards the present (Figure S1a in the Supporting Information (SI)). Given the strong isotopic discrimination during water column denitrification, the overall increase in $\delta^{15}N$ of 3‰ has been interpreted as reflecting low rates of water column denitrification during the LGM and a sharp onset of increased rates during the deglacial transition to the higher rates observed today [*Ganeshram et al.*, 2002; *Altabet et al.*, 2002; *De Pol-Holz et al.*, 2006].

[5] Reconstruction of the past $\delta^{15}N$ in sites distant from OMZ, such as the oligotrophic South China Sea [*Kienast*, 2000], reveal near-constant bulk $\delta^{15}N$ values through the last deglaciation (Figure S1b). *Kienast* [2000] interpreted these small changes as an indication that benthic denitrification changed largely in concert with water column denitrification between the LGM and the Holocene, since only a relatively fixed ratio of these two denitrification processes would ensure a relatively constant $\delta^{15}N$ of NO_3^- in regions distant from strong N-fixation and water column denitrification [*Deutsch et al.*, 2004]. In contrast, a recent study based on foraminifera test-bound $\delta^{15}N$ by *Ren et al.* [2012] shows a $\sim$ 1.2‰ glacial-to-Holocene decrease in the South China Sea.

[6] The marine $\delta^{15}N$ records provide only limited direct information on how benthic denitrification has changed across the deglaciation. Since denitrification in the sediments tends to lead to a complete utilization of NO_3^-, it is normally assumed to have no fractionation [*Brandes and Devol*, 1997], although recent studies challenged this view [*Lehmann et al.*, 2007; *Granger et al.*, 2011; *Alkhatib et al.*, 2012]. It is generally believed that benthic denitrification was likely lower during the glacial period due to lower sea-level and the resulting reduction of continental shelf area, where most of the benthic denitrification occurs today [*Middelburg et al.*, 1996; *Bianchi et al.*, 2012]. This scenario is consistent with Kienast's inference from modest changes in $\delta^{15}N$ observed in the South China Sea.

[7] The best suited records to infer glacial-interglacial changes in N-fixation stem from the Atlantic, where $\delta^{15}N$ shows a substantial LGM-to-Holocene decrease of 3‰ (Figure S1c). Given that N-fixation adds fixed N with low $\delta^{15}N$, this decrease has been interpreted to reflect an increase in N-fixation across the transition [*Ren et al.*, 2009; *Meckler et al.*, 2011].

[8] Emerging from these records is a glacial marine N cycle that operated with substantially lower rates compared to those during the Holocene. Best established are the lower rates of water column denitrification and the lower rates of N-fixation in the Atlantic, while the changes in N-fixation in the Indo-Pacific and benthic denitrification in general are less well constrained.

[9] Not well established is whether the global inventory of N was different during the LGM [*Deutsch et al.*, 2004]. Any change in this inventory requires a transient deglacial imbalance between sources and sinks of N. The magnitude of this imbalance depends on the respective strengths of the forcings impacting the N cycle and the magnitude of the negative feedbacks that reestablish a balanced cycle.

[10] N-fixation and denitrification are coupled through three negative feedbacks governed by the N:P ratio of the dissolved inorganic nutrient inventories [*Gruber*, 2004; *Deutsch et al.*, 2004; *Deutsch and Weber*, 2012]. On glacial-interglacial transition timescales, this ratio is primarily controlled by the N cycle, since the marine inventory of dissolved phosphate has a much longer residence time (50 kyr [*Delaney*, 1998] for P versus 3 to 5 kyr for N [*Eugster and Gruber*, 2012]).

[11] The first feedback involves the response of N-fixing organisms, i.e., diazotrophs, to a change in the N:P ratio (Figure 1). If the N:P ratio of the inorganic nutrient pool is lowered, diazotrophs become more competitive relative to other phytoplankton [*Karl et al.*, 2002], permitting them to increase N-fixation and thus to raise the N:P

ratio [*Haug et al.*, 1998; *Tyrrell*, 1999; *Gruber*, 2004]. The second and third feedbacks involve water column and benthic denitrification [*Codispoti*, 1989] (Figure 1). If the N:P ratio of the nutrient pool is lowered, the rate of export production will decrease due to an even stronger limitation by NO_3^-, causing a drop in export production, a lower oxygen demand from organic matter remineralization, and thus higher oxygen concentrations in the ocean interior. This decreases denitrification, permitting the N:P ratio to increase again. The strengths of these three feedbacks are poorly known, although the relatively close spatial association of N-fixation with the major denitrification zones has been interpreted as evidence that the first feedback might be quite strong [*Deutsch et al.*, 2007; *Hamersley et al.*, 2011].

[12] A series of external perturbations could have forced N-fixation and denitrification in the water column and sediments (Figure 1). For N-fixation, changes in Fe availability associated with the decrease in atmospheric dust deposition could have led to a decrease in its rates over the transition [*Falkowski*, 1997; *Broecker and Henderson*, 1998]. At the same time, the increase in the surface ocean concentration of CO_2 caused by the increase in atmospheric CO_2 could have led to higher N-fixation rates in the Holocene [*Hutchins et al.*, 2007]. Changes in water column denitrification are primarily affected by the observed increase in the extent of suboxia across the deglaciation [*Jaccard and Galbraith*, 2012], while for benthic denitrification, the changes in export production and the sea-level rise are the most important drivers [*Bard et al.*, 1990; *Hanebuth et al.*, 2000].

[13] *Deutsch et al.* [2004] investigated the strengths of the N forcings and feedbacks and their implications for the N inventory across the deglaciation using a simple geochemical box model. They varied a series of parameters associated with two forcings, i.e., extent of suboxia and sea level, and three feedbacks associated with N-fixation and denitrification in the water column and sediment and demonstrated that the $\delta^{15}N$ data from the OMZ and the mean deep ocean are well reproduced, with water column denitrification being the primary process forced by the climatic transition and N-fixation responding strongly to this perturbation. Such strong negative feedbacks tended to limit excursions in the N inventory, implying that it was unlikely more than 30% larger relative to the Holocene, with a most likely estimate of 10%.

[14] Here, we revisit the conclusions of *Deutsch et al.* [2004] using a spatially extended version of their box model as recently developed by *Eugster and Gruber* [2012]. This new box model separately considers the Southern Ocean and the Atlantic, permitting us to compare our model results also with the records from the Atlantic [*Ren et al.*, 2009; *Meckler et al.*, 2011], which was previously not possible. Like *Deutsch et al.* [2004], we investigate the response of the N cycle to forcings and feedbacks across the deglaciation but employ a state-of-the-art optimization procedure to estimate the strengths of these forcings and feedbacks. We use the same idealized formulations as *Deutsch et al.* [2004] but include two new forcings on N-fixation associated with the change in Fe availability and atmospheric CO_2. We will show that these changes lead to rather different conclusions about the size of the change in the inventory of N across the last deglaciation.

2. Method

[15] Our data-assimilation study builds on three pillars: (i) a box model of the marine N cycle (section 2.1), (ii) a set of four idealized climate forcings on N-fixation and denitrification, and three negative feedbacks between NO_3^- and N-fixation and denitrification (section 2.2), and (iii) a genetic algorithm to determine the set of seven parameters that minimize the model-data misfit (section 2.4).

2.1. Structure of the Model

[16] The model is based on the biogeochemical 14-box model recently developed by *Eugster and Gruber* [2012] (Figure 2) and resolves the Atlantic Ocean (divided into a northern and a low-latitude part), the Southern Ocean, and the joint Indian and Pacific Oceans. The Indo-Pacific is divided into an oxic and a suboxic part, with the suboxic part representing the OMZ in the Arabian Sea and the Eastern Tropical North and South Pacific. The lower thermocline box of the OMZ regions represents the suboxic volumes. Ocean transport and mixing is represented in the model by advection and mixing fluxes. Among the 2500 circulation configurations developed by *Eugster and Gruber* [2012], the setup with the smallest model-data misfit was selected here (Figure S2).

[17] The model includes all relevant marine N cycle processes and also simulates the cycling of the ^{15}N isotope (see SI for all details concerning the model). Only NO_3^- and its ^{15}N isotopic value, $^{15}NO_3^-$, are explicitly simulated, with N-fixation representing the dominant source and denitrification the dominant sinks of NO_3^-. Water column denitrification is restricted to the suboxic box of the Indo-Pacific Ocean, while benthic denitrification occurs in all basins. N-fixation occurs only in the surface boxes.

[18] The rates of the N cycle processes for the Holocene estimated by the budget approach of *Eugster and Gruber* [2012] are used as a starting point for our simulations. This cycle is balanced by construction: N-fixation releases

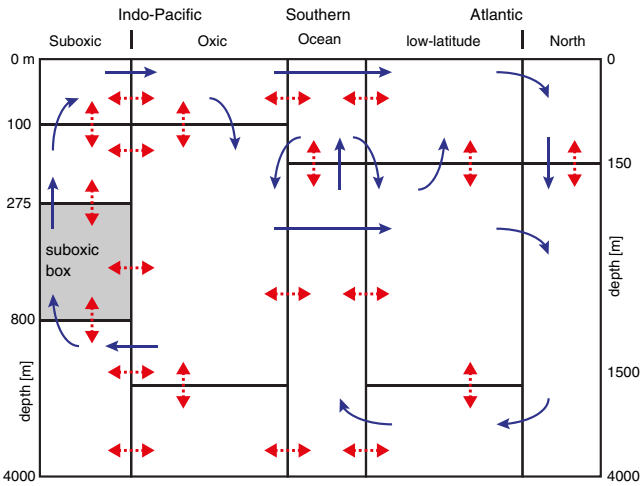

Figure 2. Schematic representation of the geochemical box model developed by *Eugster and Gruber* [2012]. Single arrows represent one-way (advection) fluxes, and double arrows two-way (mixing) fluxes. For a more detailed schematic of the box model, see Figure S2 in the SI.

164 TgN yr^{-1} of newly fixed N, and water column and benthic denitrification consume 62 and 115 TgN yr^{-1}, respectively. These rates compare well with recent estimates [e.g., *DeVries et al*. 2012]. Atmospheric deposition and river input bring 14 TgN yr^{-1} each, while sediment burial is a sink of 14 TgN yr^{-1}.

[19] Water column denitrification is implemented with a strong isotopic enrichment factor (ϵ_W = –25‰ [*Cline and Kaplan*, 1975; *Brandes et al.*, 1998]), while benthic denitrification is assumed to have no fractionation (ϵ_B = 0‰ [*Brandes and Devol*, 1997]. Isotopic fractionation through NO_3^- assimilation by phytoplankton is included with ϵ_{Norg} = –5‰ [*Sigman et al.*, 1999]). Nitrogen removed through sediment burial undergoes no isotopic fractionation [*Brandes and Devol*, 2002]. Diazotrophs release newly fixed N with an isotopic composition $\delta^{15}N$ = 0‰ [*Carpenter et al.*, 1997], and atmospheric N deposition has a $\delta^{15}N$ of –4‰, and river input discharge a $\delta^{15}N$ of 4‰ [*Brandes and Devol*, 2002].

2.2. Deglaciation Simulations

[20] For the deglacial simulations, the static model of *Eugster and Gruber* [2012] is made dynamic by scaling the Holocene rates of N-fixation and denitrification in the water column and sediments in response to a set of four idealized forcings and three feedbacks, each of which is characterized by a single parameter.

[21] More specifically, the temporally evolving rates for N-fixation (F) and water column (W) and benthic (B) denitrification in box i are computed by scaling the interglacial (I) (i.e., Holocene) by a factor consisting of the sum of three terms: (i) a scaling term S_x^y that ensures that the rates are equal their Holocene rates at time t = I, (ii) a negative feedback term that is proportional to the deviation of the N concentration in the surface (s) from its glacial (G) initial state, thereby mimicking the role of the N:P ratio in controlling the N cycle, and (iii) normalized forcing functions ($H(t)$, $L(t)$, $D(t)$, $C(t)$) that represent the impact of different climate-related forcings on the N cycle. This gives the following:

$$
\begin{aligned}
W^i(t) &= W_I^i \left(S_W^i + \alpha \frac{\mathrm{N^{i,s}}(t) - \mathrm{N_G^{i,s}}}{\mathrm{N_G^{i,s}}} + \lambda\, H(t) \right) \\
B^i(t) &= B_I^i \left(S_B^i + \beta \frac{\mathrm{N^{i,s}}(t) - \mathrm{N_G^{i,s}}}{\mathrm{N_G^{i,s}}} + \phi\, L^i(t) \right) \\
F^i(t) &= F_I^i \left(S_F^i - \gamma \frac{\mathrm{N^{i,s}}(t) - \mathrm{N_G^{i,s}}}{\mathrm{N_G^{i,s}}} \right) \\
&\quad - F_I^i(\rho_1(1 - D(t)) - \rho_2\, C(t))
\end{aligned}
\tag{1}
$$

where α, β, and γ are the parameters that determine the strengths of the feedbacks, and where λ, ϕ, ρ_1, and ρ_2 are the parameters that determine how strongly each forcing impacts the different N-processes (Figure 1, Table S1).

[22] The forcing functions, $H(t)$, $L(t)$, $D(t)$, and $C(t)$, reflect four distinct potential climate-related processes that may affect N-fixation and denitrification in the water column and sediments. Analogous to *Deutsch et al.* [2004], each of them is implemented in an idealized manner with a simple time function (Figure 1).

[23] The forcing on water column denitrification, $H(t)$, is assumed to represent the expansion of the OMZ that occurred in the middle of the deglacial transition and that gave rise to an abrupt increase in the $\delta^{15}N$ from the OMZ cores (Figure S1a). Although $\delta^{15}N$ records show different timing in the Arabian Sea and in the ETSP, a step function was chosen for $H(t)$, centered at 15.5 kyr B.P. (before present) when laminations in the Eastern Tropical Pacific began [*Keigwin and Jones*, 1990].The forcing on benthic denitrification, $L(t)$, follows the deglacial rise in sea level, which is equivalent to assuming that the area of shallow sediments is the primary factor controlling global benthic denitrification. Our model includes two forcings on N-fixation: $D(t)$ that is modeled to represent the impact of Fe availability on N-fixation [*Falkowski*, 1997; *Karl et al.*, 2002], and $C(t)$ that aims to represent the positive impact of elevated CO_2 on N-fixation [*Hutchins et al.*, 2007]. Assuming that the surface Fe concentration available for N-fixers is governed ultimately by the amount of Fe deposited onto the ocean by dust, we model $D(t)$ after the dust concentration record from the Vostok ice core [*Petit et al.*, 1999]. The carbon forcing, $C(t)$, is constructed based on the atmospheric CO_2 reconstruction from the same ice core.

[24] Three negative feedbacks between changes in export production, N-fixation, and denitrification are included in the model. These feedbacks are linked to changes in surface N, which is equivalent to linking them to the N:P ratio of the surface nutrient concentrations, as we assume a constant P cycle in the model. These feedbacks are formulated in such a way that they represent the impact of changes in primary and export production on the marine N cycle even though these changes are not explicitly modeled. Specifically, these feedbacks encapsulate the concept that changes in the surface ocean NO_3^- alter (i) the competitivity of diazotrophs, and thus the rates of N-fixation, and (ii) primary and export production, and thus the rates of denitrification in the water column and sediments. This permits the model to incorporate changes in export production in an implicit manner through a perturbation approach, even though the explicitly modeled "background" export production is kept constant across the deglaciation.

[25] The initial glacial rates of the N fluxes, the N inventories, and the $\delta^{15}N$ in each box were computed analytically in such a way that Holocene fluxes and inventories are reached when the model is run forward in time across the deglaciation. This gives a quadratic system of 14 equations, which was solved by a gradient method (SI B and C).

[26] x'Several assumptions were made in the construction of our model and our simulations. These include (i) constant background export production, (ii) constant P inventory, (iii) balanced N budgets in the glacial and Holocene, (iv) invariant ocean transport and mixing across the deglaciation, and (v) no change in atmospheric deposition, river discharge, and sediment burial of N. Some of these assumptions are well justified or are likely not of importance. Others were made to simplify the model or because the available evidence is insufficient to develop a more realistic scenario. We will discuss the implications of these assumptions in section 5.2.

2.3. Data Constraints

[27] Simulated δ^{15}N are compared with records at three sites: the OMZ, the oxic Indo-Pacific, and the low-latitude Atlantic. Three idealized records were generated for each site from the original records (see caption of Figure 3 for sources) by temporally smoothing them with a moving-average filter with a filter-width of 4 kyr (Figure 3). The different records were shifted in order to account for spatial variations (Figure S1a).

[28] The three idealized δ^{15}N records are used as constraints for the modeled δ^{15}N of NO_3^- in three distinct boxes. The OMZ δ^{15}N record is assigned as a constraint for the surface box of this region, that of the South China Sea is related to the deep box of the oxic Indo-Pacific, and the Atlantic records constrain the δ^{15}N of NO_3^- in the thermocline box of the low-latitude Atlantic. The selection of the individual boxes is based on the following arguments. In the case of the OMZ, the isotopic composition of the sinking organic nitrogen corresponds directly to the isotopic composition of the NO_3^- in the surface ocean. This is a consequence of a nearly complete utilization of the upwelled NO_3^- in this region [*Thunell et al.*, 2004]. We use a deeper box for the oxic Indo-Pacific, as the exchange with the surface is restricted and the δ^{15}N of the exported organic nitrogen obtains the value of the box supplying the surface with NO_3^-, i.e., the δ^{15}N of NO_3^- of the North Pacific deep water, since the characteristics are similar to those in the South China Sea [*Wong et al.*, 2007]. The thermocline box of the Atlantic is used following similar arguments and because the N contained in foraminifera ultimately stems quantitatively from the NO_3^- in the thermocline, as this is the most important source of fixed N for the surface ocean.

[29] The use of δ^{15}N of organic matter as a constraint for the modeled δ^{15}N of NO_3^- is potentially problematic, as (unrecognized) incomplete utilization and fractionation processes within the ecosystem might lead to substantial offsets between the two pools [*Somes et al.*, 2010]. Ideally, one would formulate the model's cost function in terms of δ^{15}N of organic matter, but our model does not explicitly model this component. However, we regard the potential errors and uncertainties from our choice as relatively small, since the paleoceanographic records generally have been obtained from sites where the effective offset between the δ^{15}N of NO_3^- and that of organic matter is minimal.

2.4. Optimization

[30] A genetic algorithm is adopted to perform the optimization of the seven parameters (detailed description in the SI D, see also Figure S4). This method was chosen in order to ensure the identification of a global minimum of the cost function, which is difficult to achieve for such highly nonlinear problems. Tests with different initial conditions showed good convergence.

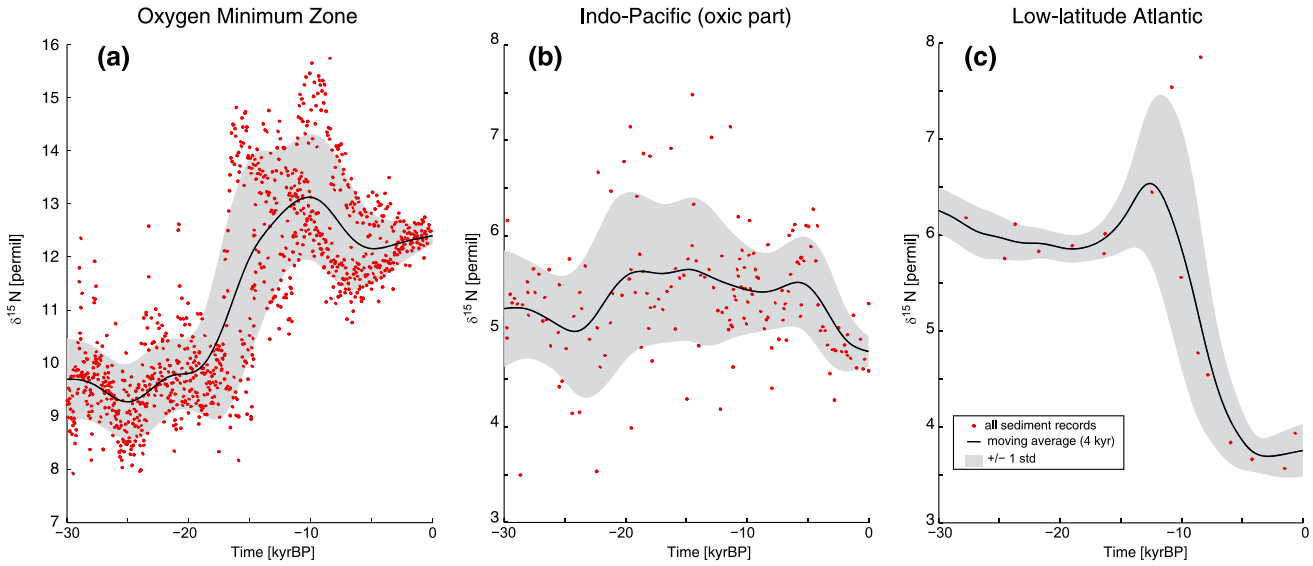

Figure 3. Idealized downcore bulk and foraminifera test-bound δ^{15}N records generated by shifting raw data (see Figure S1 in the SI) such that the current interglacial δ^{15}N are in line with the modeled value at this time at each site. (a) δ^{15}N data of OMZ [to be compared with suboxic surface box]; (b) the South China Sea [deep box of the oxic Indo-Pacific]; and (c) the Caribbean Sea and the Gulf of Mexico [thermocline box of the low-latitude Atlantic]. Black line, moving average with a timespan of 4 kyr; gray zone, one sample standard deviation. References: OMZ: δ^{15}N of bulk organic matter from sediment cores RC27-14 and RC27-23 on the Oman continental margin [*Altabet et al.*, 2002], core 905 in the southwestern Arabian Sea [*Ivanochko et al.*, 2005], and core GeoB 7139-2 off northern Chile [*De Pol-Holz et al.*, 2006]. Oxic Indo-Pacific: four downcore records of bulk sediment δ^{15}N of the South China Sea [*Kienast*, 2000]. Low-latitude Atlantic: Foraminifera test-bound δ^{15}N of *Orbulina universa* from ODP 999A located in the Caribbean Sea [*Ren et al.*, 2009] and *O. universa* from giant box core MD02-2550 from the Orca Basin in the Gulf of Mexico [*Meckler et al.*, 2011].

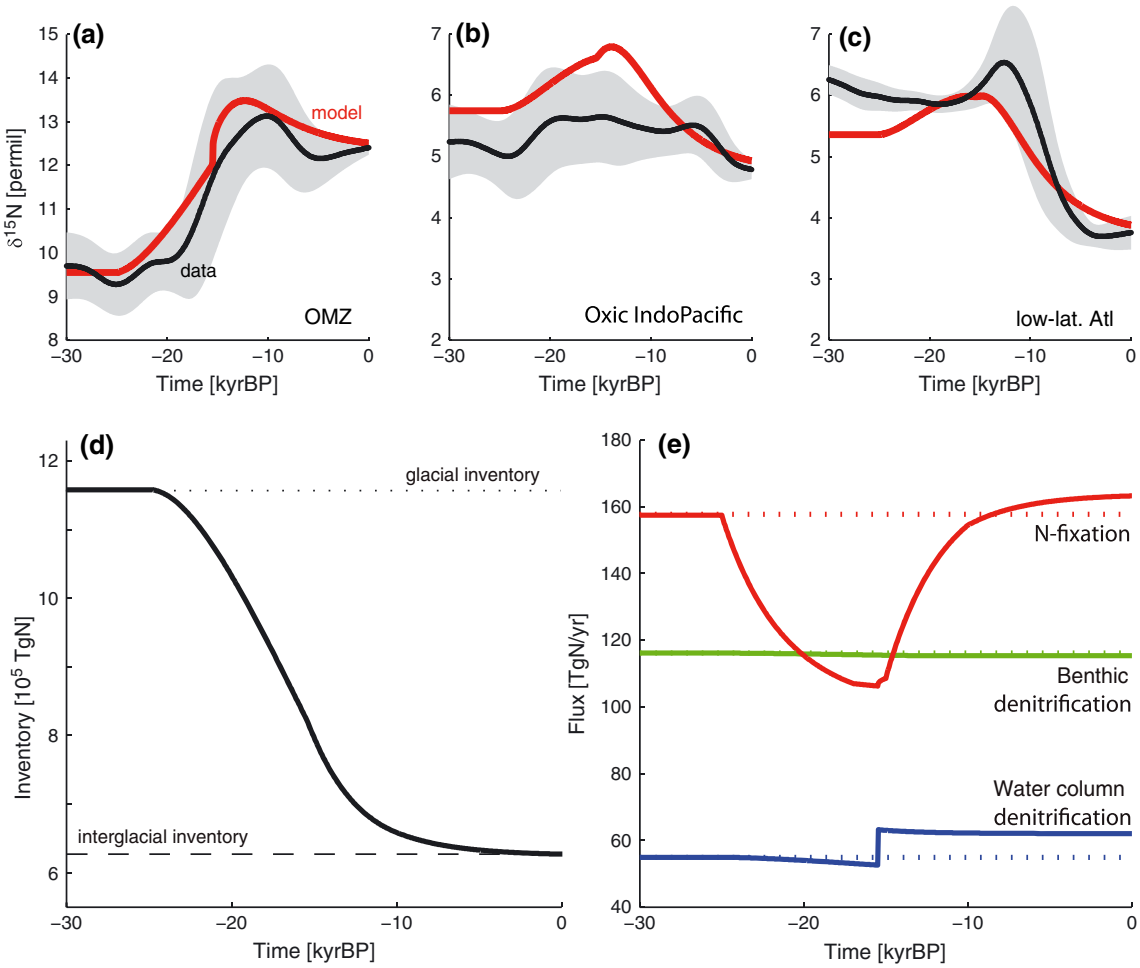

Figure 4. δ^{15}N constraints are as follows: (a) OMZ, (b) deep oxic Indo-Pacific, and (c) low-latitude Atlantic thermocline. (d) The global N inventory for the standard case; (e) N-fixation and water column and benthic denitrification trajectories across the last glacial termination for the standard case.

3. Deglacial Changes in the N Cycle

[31] The optimized model manages to fit the δ^{15}N data from all three sites with regard to both timing and magnitude (Figure 4; see also SI E and Figure S6). The best agreement is achieved for the data from the OMZ site, where the model captures the onset of the rapid increase in δ^{15}N at around 18 kyr B.P., although modeled δ^{15}N starts to increase around 25 kyr B.P., i.e., several thousand of years before the data. The model represents well the maximum around 12 kyr B.P. and also simulates the subsequent decrease into the Holocene in accordance with the observations. The model suggests a deglacial δ^{15}N peak in the oxic Indo-Pacific which is not observed in the *Kienast* [2000] data used here (Figure 4b). Nevertheless, the glacial and Holocene data from the oxic Indo-Pacific are well modeled. The transition is less well captured, with the model simulating a too strong maximum in δ^{15}N around 12 kyr B.P., although the model is only slightly outside the uncertainty band of the data (Figure 3b). Data from the subtropical Atlantic are the least well captured; the model underestimates the magnitude of the LGM-to-Holocene decrease of δ^{15}N and also simulates a too early deglacial maximum.

[32] These fits are achieved by the model identifying substantial changes in the marine N cycle across the deglaciation. In particular, our standard model suggests a 46% decrease in the global inventory of N across the transition (Figure 4d). This large decrease in the N inventory starts before 20 kyr B.P. and continues relatively monotonously until the current interglacial inventory is reached $\sim$ 10 kyr B.P.

[33] This decrease in the N inventory is a consequence of a large transient source-sink imbalance, which is driven by a temporary reduction in N-fixation that lasts over several thousand years (Figure 4e). N-fixation starts to decrease at around 25 kyr B.P. due to a diagnosed strong response of this process to global decreasing inputs of dust (Figure 1). The value of the corresponding parameter (ρ_1) is by far the largest of all forcing parameters in this standard case (Table S1). The next forcing in the deglacial sequence is sea-level rise acting upon benthic denitrification, but the optimized model suggests that the strength of this forcing (ϕ) is very weak. Also, the strength (β) of the feedback associated with this sink is weak, and therefore this sink process is diagnosed to have remained nearly unchanged across the deglaciation. N-fixation decreases by 33% until $\sim$15.5 kyr B.P., whereupon it begins to increase rapidly. This

late deglacial increase occurs primarily due to a diagnosed strong N-fixation feedback (γ) reacting to the step function increase in water column denitrification (λ), whose shape we prescribed to mimic the rapid increase in anoxia thought to have taken place around this time ($H(t)$, Figure 1). This increase in water column denitrification decreases the surface ocean N:P beyond the level already achieved by the long-term decrease caused by the low N-fixation rates that prevailed the preceding millennia. Before this step increase, a slight decrease in water column denitrification is observed since this sink is sensitive to local change in surface N:P ratio due to the feedback associated with the decreasing N inventory (see equation (1)). Further affecting the late deglacial increase in N-fixation is the forcing associated with increasing levels of CO_2 (ρ_2). In the end, N-fixation increases slightly (4%) between the last glacial period and the Holocene.

[34] The drivers for the glacial-to-Holocene change in the N inventory can be directly evaluated on the basis of the analytical equation that was used to compute the glacial initial state (see SI B2). If we sum over all boxes, a good approximation of the relative change in the N inventory across the deglaciation is

$$\frac{\Delta \mathrm{N}}{\mathrm{N_G}} \approx -\frac{\lambda\, W_I + \phi\, B_I + (\rho_1 - \rho_2) F_I}{\alpha\, W_I + \beta\, B_I + \gamma\, F_I}. \qquad (2)$$

This means that the glacial-to-Holocene change in the N inventory is directly related to the ratio of the flux weighted forcing strengths over the flux weighted feedback strengths. With the interglacial rates, $F_I \approx W_I + B_I$, and our findings of $\rho_1 \gg \lambda, \phi, \rho_2$ and $\gamma \gg \alpha, \beta$ (Table S1), equation (2) simplifies to

$$\frac{\Delta \mathrm{N}}{\mathrm{N_G}} \approx -\frac{\rho_1}{\gamma}, \qquad (3)$$

which means that the magnitude of the decrease of the inventory is almost entirely determined by the ratio of ρ_1 associated with the dust forcing acting on N-fixation and the strength of the N-fixation feedback, γ, highlighting the crucial role of N-fixation in driving the deglacial N cycle changes.

[35] The global changes are mirrored in the individual ocean basins, although with distinct spatial differences (Figure S8). This basin-scale analysis comes with a caveat, though, as our assuming constant circulation likely has a larger impact at the basin-scale results compared to the global scale. Notwithstanding this caveat, our model diagnoses a substantially larger increase in N-fixation across the deglaciation in the oxic Indo-Pacific compared to the North Atlantic. The low-latitude Atlantic and OMZ regions follow the global mean, but N-fixation decreases in the Southern Ocean by ~30%. Following *Eugster and Gruber* [2012], we have little confidence in the N-fixation rate in the Southern Ocean because the pre-industrial rate was estimated under the assumption that phytoplankton take up N and P following the Redfield ratio, while *Weber and Deutsch* [2010] reported that non-N-fixing organisms uptake is non-Redfieldian there. This result, in turn, implies that the estimate of the rate of N-fixation in this region is likely biased.

[36] The picture that emerges from the standard case is one of a rather dynamic marine N cycle across the deglaciation and one that is largely driven by a strong temporary dip in N-fixation. This reduction leads to a large temporal imbalance that is diagnosed to occur in all ocean basins leading to a near-halving of the N inventory across the transition. The dip in N-fixation is driven by a strong response of N-fixation to a decrease in dust forcing, but it needs to be emphasized that the model does not explicitly consider Fe limitation for N-fixation. Rather, it diagnoses a response to a climate-related forcing that has a temporal evolution similar to that of dust. The direct implication of this finding is that N-fixation ultimately drives the overall N inventory changes across the last deglaciation in our model.

4. Sensitivity Analyses

[37] It is critical to evaluate the robustness of our results and to better understand the impact of some of the assumptions that form the basis of our data-assimilation study. Of particular relevance is that our results, especially our finding of a glacial N inventory that was nearly 100% larger than that of the Holocene, differ substantially from those of *Deutsch et al.* [2004]. They argued that the glacial inventory was most likely less than 10% larger.

[38] To determine the reasons for these differences, we mimic the model setup of *Deutsch et al.* [2004] by turning off the iron and carbon forcings on N-fixation and fitted the model only to δ^{15}N records assigned to the OMZ and the oxic Indo-Pacific (considered as reflecting the mean ocean in the *Deutsch et al.* [2004] model). In this Deutsch-like model case, the N inventory decrease between glacial and Holocene is indeed much smaller than in our standard case (–19% instead of –46%) and close to Deutsch's estimate of at most –30% and most probable of –10% (comparison and detailed discussion in the SI F). While this Deutsch-like model fits the δ^{15}N records in the OMZ and the oxic Indo-Pacific nearly as well as our standard model, it fails to simulate the observed LGM-to-Holocene decrease in δ^{15}N in the low-latitude Atlantic. Thus, the inclusion of these new data into our assimilation requires the model solution to shift substantially. The addition of the dust forcing is clearly important as well, since without this forcing, N-fixation cannot drive the N cycle across the transition. Rather, it can only respond to the changes in denitrification.

[39] In the next series of experiments, we tested for the sensitivity of our model results to the data constraints (see SI G). The most sensitive cases are associated with the strongest weighting of the data from the OMZ (weighting factor ω) relative to the other sites (Figure S10). When the OMZ data are given 0.1 times the weight of the other regions, the inventory reduction is only 16%, while in the case of the strongest weight (ω = 10), the reduction is close to that of the standard case, i.e., 47%. In contrast to the high sensitivity of the weighting of the data from the OMZ, the relative weight given to the data from the oxic Indo-Pacific matters little (Figure S10). Thus, the uncertainties associated with the sediment record by *Kienast* [2000], used to represent this region, have only a small influence on our results. Also, the amount of smoothing of the data used to constrain the OMZ has relatively little influence on the results.

[40] Most cases where we changed the timing or shape of the external forcings resulted in similarly large deglacial reductions of the N inventory as was the case in the standard case. An important exception is the case where we

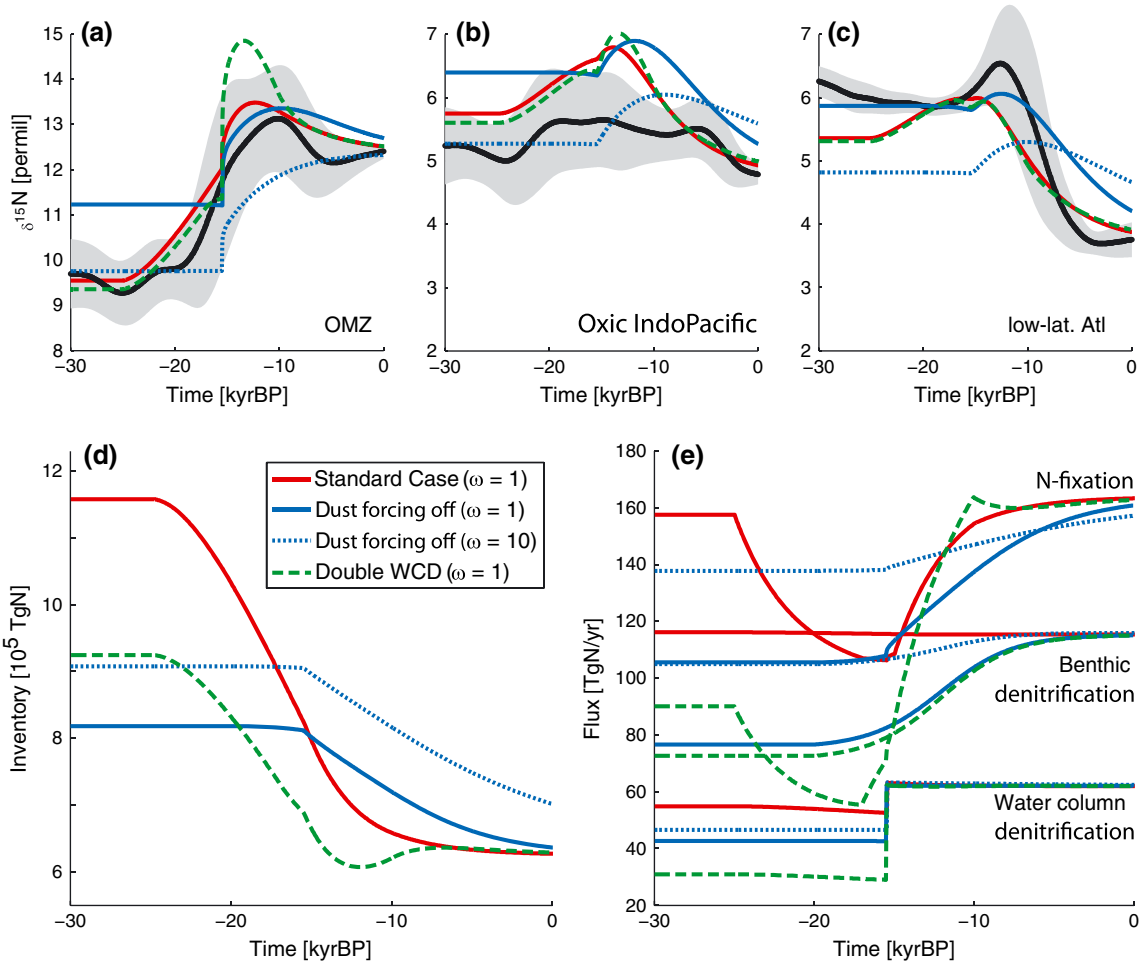

Figure 5. Sensitivity analyses toward the external forcings: standard case; case where the dust forcing affecting N-fixation is turned off and with the OMZ weighting factor, ω, of 1 or 10; and case with water column denitrification forced to double across the deglaciation. δ^{15}N constraints are (a) OMZ, (b) deep oxic Indo-Pacific, and (c) low-latitude Atlantic thermocline. (d) Global inventory of N; (e) N-fixation and water column and benthic denitrification across the last deglaciation.

turned dust forcing off (see Figure 5 and SI H). In this case, N-fixation, by design, does not take an early deglacial dip. It increases during the second half of the deglaciation in response to an increase in denitrification in the water column and sediments that are diagnosed to increase more strongly than in the standard case. However, the fit of the model to the data is much worse than in the standard case, with the model strongly underestimating the deglacial increase in δ^{15}N in the OMZ. A further case with dust forcing turned off, where we gave more weight to the OMZ data to force a better fit there, resulted in the model underestimating the deglacial drop in the δ^{15}N in the low-latitude Atlantic.

[41] The timing of the dust forcing matters for the model as well but only with regard to the temporal evolution of the changes, while the total loss of N across the deglacial is about the same as in the standard case (see Figure S12). This case is relevant since we may have prescribed the dust forcing to decline too early in our simulations because of using dust concentrations rather than dust fluxes to determine the onset [*Petit et al.*, 1999]. Our sensitivity analyses show that the later the dust forcing starts, the later N-fixation starts to decline but also the deeper is the diagnosed reduction in N-fixation. This leads in all cases to nearly the same imbalance of the N-budget and hence to nearly the same overall decrease in the N inventory.

[42] Our results are also not very sensitive to the shape of the suboxia forcing. The model gives results very similar to the standard case in a case where the change in suboxia is more gradual instead of abrupt and even when it is entirely omitted (Figure S11). We thus conclude that the timing of the forcing and its exact shape has overall only a small impact on the diagnosed decrease in the N inventory.

[43] Another key finding from our standard case is that the rates of the key N-processes are nearly identical at the LGM relative to the Holocene. This differs from the generally accepted view of lower glacial rates (see section 1). To challenge our model, we run a sensitivity case where we forced the model to have a rate of water column denitrification during the LGM that is half of that in the Holocene. The resulting modeled δ^{15}N fit the observational constraints in the oxic Indo-Pacific and the subtropical Atlantic nearly identically to the standard case and make the fit in the OMZ only slightly worse by generating a too high maximum around 13 kyr B.P. (Figure 5). This scenario generates,

however, a smaller decrease in the N inventory of about –32% but still larger than postulated by *Deutsch et al.* [2004].

[44] In summary, the sensitivity analyses reveal that the diagnosis of a temporary deglacial imbalance between sources and sinks that leads to a loss of N in the ocean between the LGM and the Holocene of 16 to 50% is a robust finding within the context of our box model. Also robust is that this imbalance is primarily caused by a dip in N-fixation that is diagnosed to occur in response to a decrease in the input of iron-rich dust that begins in the very early part of the deglacial transition and ends around 15 kyr B.P., when N-fixation begins to respond very quickly to the onset of enhanced water column denitrification. We will show below that this conclusion even holds for a case where ocean circulation is altered over the course of the deglaciation. Less robust are the diagnosed rates of N-fixation and denitrification in the water column and sediments for the LGM. Solutions with roughly equal rates between the LGM and Holocene produce only a marginally better fit to the data constraints compared to solutions where the rates at the LGM are about half as large as during the Holocene. This is an implication of the ocean's mean $\delta^{15}N$ providing a constraint only on the ratio of water column to benthic denitrification, but not on the total rate [*Brandes and Devol*, 2002; *Deutsch et al.*, 2004].

5. Discussion

[45] Our results raise a number of questions we address in turn. First, why is the model diagnosing an early deglacial reduction in N-fixation and consequently a substantial decrease in the marine N inventory across the last deglacial? Second, what are the impacts of some of the simplifying assumptions we made in developing our model? Third, how can we rationalize our findings and connect them with what we know about the biogeochemical controls on the marine N cycle? The fourth and final question is what are the implications of our diagnosed high-N ocean during the LGM upon ocean productivity, export production, and ultimately atmospheric CO_2?

5.1. What Drives the Results?

[46] Our finding of N-fixation dominating the dynamics of the glacial transition in the marine N cycle is particularly puzzling because none of the $\delta^{15}N$ records show major changes before about 18 kyr B.P., at a time when most of the dip in N-fixation had already occurred in our model. Furthermore, the Atlantic $\delta^{15}N$ records show a clear overall LGM-to-Holocene decrease, which consistently has been interpreted as the Holocene supporting higher rates of N-fixation compared to the LGM [*Ren et al.*, 2009; *Meckler et al.*, 2011].

[47] Key to understanding our findings are the temporally diverging tendencies of the $\delta^{15}N$ values in the different oceanic regions (Figure 3), while the global mean $\delta^{15}N$ of NO_3^- remained relatively constant between the LGM and the late Holocene [*Altabet*, 2007]. During the LGM, the $\delta^{15}N$ of NO_3^- was nearly the same in the oxic Indo-Pacific and Atlantic, and it was only slightly higher in the OMZ, leading to a relatively homogeneous distribution. In contrast, the differences are much larger during the late Holocene, with the Atlantic having a much lower $\delta^{15}N$ of NO_3^- and the OMZ having a much higher value.

[48] The observation of a largely invariant mean ocean $\delta^{15}N$ of NO_3^- requires that the fraction of denitrification occurring in the water column must have remained roughly the same as well, as any change in this ratio would alter this value [*Kienast*, 2000; *Brandes and Devol*, 2002; *Deutsch et al.*, 2004]. This leaves only two processes that can be changed through the deglaciation: (i) the total rates of denitrification (or N-fixation in steady state) and (ii) the total inventory of N.

[49] If we assume for the moment an invariant N inventory, the observed strong increase in the $\delta^{15}N$ in the OMZ requires a strong increase in water column denitrification and a corresponding increase in sediment denitrification to keep the fraction of total denitrification occurring in the sediments constant (see detailed discussion in SI I and Figure S13a). Such an increase in denitrification would not alter much the $\delta^{15}N$ of the oxic Indo-Pacific (Figure S13b), in agreement with the observations by *Kienast* [2000]. But it also would not alter much the $\delta^{15}N$ of the low-latitude Atlantic despite the large increase in N-fixation there needed to balance the increase in denitrification (Figure S13c). This scenario corresponds to the solution identified by *Deutsch et al.* [2004], and as this one, it fails to fit the Atlantic data.

[50] This is where the second process comes in, i.e., the change in inventory. A decrease of the global inventory of N, while keeping all rates constant, provides another means to increase $\delta^{15}N$ in the OMZ. But this would cause at the same time a decrease of the $\delta^{15}N$ in the oxic Indo-Pacific and in the low-latitude Atlantic (see Figures S13d–S13df, S14, and SI I). This is a result of the dilution effect introduced by *Deutsch et al.* [2004]. A smaller inventory for the same rate of water column denitrification causes the fraction of NO_3^- remaining in the OMZ to decrease, yielding a higher $\delta^{15}N$ of NO_3^-. At the same time, the concentration of NO_3^- that is mixed out and carries the isotopic signature of water column denitrification decreases as well, so that the influence of the OMZ on the mean isotopic composition of the ocean decreases, resulting in a lower mean $\delta^{15}N$ of NO_3^- outside the OMZ. On a basin-scale, it turns out that such a decrease in the N inventory has a proportionally stronger effect on the $\delta^{15}N$ in the low-latitude Atlantic compared to the oxic Indo-Pacific (Figure S13e,f).

[51] During the optimization, the model combines the two key processes in order to explain the whole LGM-to-early Holocene transition, with the exact solution critically depending on how strongly the data from the OMZ are weighted and whether additional constraints on denitrification are added. In the standard case, the model accomplishes to fit most of the observed changes in $\delta^{15}N$ by altering the N inventory with a relatively small contribution from changes in denitrification. In the cases of either weak OMZ weighting or imposed low rates of water column denitrification during the LGM, the model diagnoses a stronger contribution from denitrification, but still most of the transition is accomplished by changing the inventory (see Figures 5 and S10). The only process that can induce the reduction in the N inventory needed to simultaneously fit the data from all sites and without altering the ratio of water column to

benthic denitrification is N-fixation. Its net effect on $\delta^{15}N$ of NO_3^- is modest, permitting the model to adjust this process without altering substantially the global mean NO_3^-.

[52] The transition from the LGM to the Holocene occurs in two distinct phases: During the first phase, i.e., from ~25 kyr to ~15.5 kyr, nearly all changes in $\delta^{15}N$ need to be explained by the dilution effect and by changes in N-fixation, as the contributions from the denitrification processes cannot be important due to the lack of external perturbation acting upon them. In our standard solution, the dilution effect explains essentially all of the increase in the $\delta^{15}N$ in the OMZ until ~15.5 kyr. Absent any change in N-fixation, this would cause the $\delta^{15}N$ of the rest of the ocean to decrease (Figure S14). This is not the case, however, since the decrease in N-fixation, which causes a reduction in the addition of low $\delta^{15}N$ to the system, compensates for this decrease. In fact, it even overcompensates it, as evidenced by the mid-deglacial peak in $\delta^{15}N$ in the oxic Indo-Pacific and low-latitude Atlantic. Thus, the solution identified by the model's optimization system for the first part of the deglacial is for N-fixation to take a temporary dip, which generates the temporary imbalance needed to reduce the N inventory. This, in turn, increases the $\delta^{15}N$ of the OMZ despite constant water column denitrification, whereas the expected decrease in $\delta^{15}N$ in the rest of the ocean is counterbalanced by the isotopic effect of a decrease in the rates of N-fixation.

[53] During the second phase, i.e., from ~15.5 kyr until ~10 kyr, the contribution of the inventory change on the dilution effect is relatively small, as most of the deglacial N inventory change has already occurred (Figure 4). Instead, the subsequent changes in $\delta^{15}N$ stem from the interaction of changes in water column denitrification and N-fixation. In the OMZ, the onset of water column denitrification causes a further increase in the $\delta^{15}N$, which is later eroded away due to mixing and the global adjustment between the sources and sinks of N and of its isotopes. In the oxic Indo-Pacific and the low-latitude Atlantic, the fast recovery of N-fixation leads to a strong drop in $\delta^{15}N$, explaining most of its glacial-to-Holocene change. Thus, the second phase of the deglacial follows more closely the canonical interpretation of the deglacial changes in the marine N cycle, i.e., onset of water column denitrification followed by an increase in N-fixation.

[54] The implications of our results for the interpretation of the individual records are quite fundamental. Our model shows, for example, that the LGM-to-Holocene decrease in $\delta^{15}N$ in the Atlantic is not caused by the Holocene having much higher rates of N-fixation in this basin compared to the LGM but is because of a reorganization of the global N cycle. This involves an interacting set of changes in the global inventory, increases in denitrification, and N-fixation taking a temporary dip during the deglacial. Thus, our interpretation differs fundamentally from the hypotheses of *Ren et al.* [2009] and *Meckler et al.* [2011], who suggested a LGM-to-Holocene increase in N-fixation of up to a factor of 5.

[55] Our model also suggests that the dilution effect, regulated largely by changes in the global inventory, might have caused a large fraction of the LGM-to-Holocene increase in the $\delta^{15}N$ of the OMZ. This effect, previously little considered, strongly reduces the need for a large change in water column denitrification, which is generally invoked to explain the increase in the $\delta^{15}N$ of the OMZ [*Ganeshram et al.*, 2002; *Altabet et al.*, 2002; *De Pol-Holz et al.*, 2006]. Finally, our model also suggests a complex balance between the impacts of the dilution effect and local changes in N-fixation in explaining the relatively constant oxic Indo-Pacific $\delta^{15}N$ record. These particular conclusions are hampered somewhat by the fact that our model simulates a deglacial peak and a glacial-Holocene decrease in $\delta^{15}N$ there, i.e., features that are not shown in the $\delta^{15}N$ records by *Kienast* [2000] used to constrain the model. However, a recent foraminifera test-bound record from the South China Sea by *Ren et al.* [2012], not employed in our study, exactly shows these features, i.e., a deglacial peak in $\delta^{15}N$ and an overall ~1.2‰ glacial-to-Holocene decrease.

5.2. What Are the Impacts of the Assumptions?

[56] Global background export production, the marine P cycle, atmospheric and river inputs of N, and ocean circulation are assumed to have remained constant across the deglaciation. Furthermore, we assumed zero fractionation during benthic denitrification, while recent studies indicated that this might not be the case.

[57] The assumption of constant background export production is likely not a critical one in the context of our modeling study, as the most important impact of a variable export production on marine N is included implicitly in our feedback formulations through deviation in the local N:P ratio (see equation (1)). Furthermore, the currently available evidence suggests relatively small glacial-to-Holocene changes in global export production [*Kohfeld et al.*, 2005]. We also consider our assumption of a constant marine P cycle as relatively uncritical, primarily because the long residence time of marine P in the ocean makes this cycle rather static on the 10 kyr timescale of the deglaciation transition [*Delaney*, 1998; *Benitez-Nelson*, 2000].

[58] Changes in the inputs of N through atmospheric deposition and river discharge are also unlikely of critical importance. First, their magnitude is substantially smaller than the rates of N-fixation and denitrification, and although changes in their magnitudes are not well established, it is unlikely that they changed by more than a factor of 2. Second, the most likely scenario is that these inputs were actually smaller during the LGM, mostly because the hydrological cycle was slower and the atmosphere drier during that time [*Yung et al.*, 1996]. This would have worked against a higher N inventory in the LGM but likely only to a very limited degree.

[59] We also expect a relatively modest impact of uncertainties in our assumption of zero fractionation during benthic denitrification. If the recent results of an expressed fractionation of more than 6‰ [e.g., *Lehmann et al*. 2007, *Granger et al*. 2011, and *Alkhatib et al*. 2012] were true globally, it would primarily affect our initial conditions, particularly the relative rates of water column to benthic denitrification. We would not expect strong changes in the diagnosed deglacial evolution, unless the fractionation itself changes. Lacking evidence in support for such a change and given so far only indications from two locations, i.e., the Bering Sea and the St. Lawrence, for an expressed fractionation during benthic denitrification, we consider our assumption as relatively robust but might be forced to reevaluate it

should the canonical view of zero fractionation for benthic denitrification change.

[60] In contrast to these previous assumptions, we are concerned about the assumption of constant ocean circulation through the course of the deglacial transition. Of particular concern is the observation that the most critical region, i.e., the suboxic part of the OMZ, underwent substantial changes in ventilation both as a result of the general reorganization of the oceanic circulation between the LGM and the Holocene as well as in response to millennial scale abrupt changes [*Galbraith et al.*, 2004; *Jaccard and Galbraith*, 2012; *Schmittner and Galbraith*, 2008]. Any change in the ventilation of the suboxic volume of the OMZ has direct implications for the global $\delta^{15}N$ of NO_3^-, as it changes the magnitude of the dilution effect. A higher ventilation, i.e., shorter residence time, of waters in the suboxic volume is fundamentally equivalent to an increase in the N inventory with regard to its effect on the global distribution of $\delta^{15}N$ of NO_3^-, as it decreases the degree to which NO_3^- supplied to this volume is denitrified. Thus, a deglacial decrease in the ventilation of the OMZ, as suggested by the expansion of hypoxia [*Jaccard and Galbraith*, 2012], while keeping denitrification rates constant, represents an alternative means to induce the increase in $\delta^{15}N$ observed in the OMZ regions, the near constancy of $\delta^{15}N$ in the oxic Indo-Pacific, and the decrease in $\delta^{15}N$ in the Atlantic. A sensitivity case where we increased the mixing term in the anoxic volume of the OMZ by several orders of magnitude showed, however, that the contribution of circulation change is likely insufficient to generate the observed changes in $\delta^{15}N$. Nevertheless, such a ventilation decrease in the OMZ has an impact on the magnitude of the N inventory decrease needed to fit the data, making our standard case an upper estimate of the N inventory change.

[61] Changes in ocean circulation might also affect our diagnosed N-fixation rates, especially in the Atlantic Ocean, where ocean circulation was clearly different during the LGM [*Duplessy et al.*, 1988; *Lynch-Stieglitz et al.*, 2007]. In particular, the mid-depth circulation was dominated at that time by Glacial North Atlantic Intermediate Water (GNAIW) [*Gherardi et al.*, 2009], which replaces southern-sourced waters throughout much of the upper Atlantic. As a result, this region was probably more geochemically isolated during the LGM compared to today, especially with regard to the transport of low N:P waters from the Indo-Pacific and the Southern Ocean into the subtropical and northern Atlantic. The implications for this in our data-assimilation setup are difficult to fathom, but we expect a smaller deglacial dip and perhaps a stronger late glacial rise in N-fixation.

5.3. How Can We Rationalize the Results?

[62] The picture that emerges is a deglacial change in the marine N cycle driven largely by N-fixation, with changes in denitrification being of lesser importance. Particularly compelling is our finding that the rates of N-fixation could have been about the same during the LGM compared to those during the late Holocene. How can these dynamics of N-fixation be rationalized given our current knowledge of the working and controls of the marine N cycle?

[63] We aim to explain the evolution of N-fixation as follows (see also Figure 6): In a high-N glacial ocean, marine

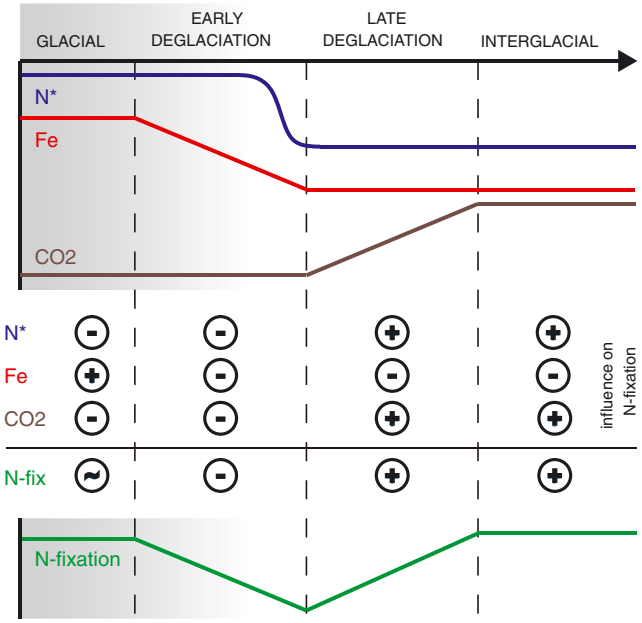

Figure 6. Proposed scenario for the dynamics of N-fixation influenced by N^*, input of iron from atmospheric dust deposition and atmospheric CO_2. The last glacial termination is divided into a glacial, an early deglacial, a late deglacial, and the current interglacial (Holocene) periods. Changes in N^*, iron input, and carbon level (upper part of the figure) and how these factors favor ($\oplus$) or restrict ($\ominus$) N-fixation (middle part). Variation in N-fixation depends on the individual participation of N^*, the iron input, and the atmospheric CO_2, with the assumption that carbon has the potential to influence the iron requirement of diazotroph (lower part).

diazotrophs would have been in a situation of very strong competition, as their most important niche, i.e., waters with low NO_3^- but high PO_4^{3-} and therefore high N^* ($N^* = NO_3^- - 16\,PO_4^{3-} + 2.9$ mmol m^{-3}), would have been rare. However, the enhanced availability of iron would have permitted the N-fixers to remain competitive [*Paerl et al.*, 1994; *Monteiro et al.*, 2011; *Dutkiewicz et al.*, 2012] and enable them to maintain relatively high rates of N-fixation. However, when the input of dust began to decrease around 25 kyr B.P., N-fixers quickly became disadvantaged in comparison to the other phytoplankton because of their relatively high demand for iron. As a result, N-fixation rates began to fall. This trend continued throughout most of the first half of the deglaciation, until when water column denitrification increased in the OMZ regions, leading to a rapid local decrease in the relative abundance of NO_3^- versus PO_4^{3-}. This widened the niche for diazotrophs substantially, permitting them to outcompete the other phytoplankton in these regions despite the iron stress. This development was strengthened further by the continuing decrease of the N inventory, which led to a global-scale widening of the niche for the diazotrophs in the second half of the deglaciation. Further assisting this rebound of the N-fixers was the increase in atmospheric CO_2, which stimulated their growth. By the time the Holocene was reached, diazotrophs had fully rebounded in their rates to the LGM levels.

[64] Although the overall (global) rates of N-fixation are similar between the LGM and the Holocene, the controls have changed fundamentally. According to our scenario, the N-fixation rates were primarily controlled by the competition with other phytoplankton during the LGM and possibly by CO_2 (in the model there is only an implicit influence of CO_2 on the rates of N-fixation). In the Holocene, the competition is less severe, as there are many regions with low NO_3^- and high PO_4^{3-} concentrations, giving them a high relative fitness. But iron levels are low, making it a proximate limiting factor.

5.4. What Are the Implications of the Results?

[65] The biogeochemical implications of a high-N ocean during the LGM depend on two elements: (i) the phosphorus inventory and (ii) the N:P ratio of phytoplankton. If the P inventory increased commensurably with that of fixed N, primary and export production should have been much larger during the LGM, making the biological pump an important contributor to the drawdown of atmospheric CO_2. *Archer et al.* [2000] estimated that a 50% increase in the marine N inventory (assuming that P is not becoming limiting) would have decreased atmospheric CO_2 by about 50 ppm. If the P inventory remained unchanged, then the N:P and the C:P ratios of phytoplankton would need to have been larger in order to increase primary and export production.

[66] Historically, the possibility of a substantially higher P inventory during the LGM was discarded on the basis of the long residence time of P in the ocean. However, a number of recent studies suggested that the residence time is much shorter and that the LGM inventory of P was indeed higher than the pre-industrial one [*Ganeshram et al.*, 2002; *Tamburini and Foellmi*, 2009; *Wallmann*, 2010]. But the evidence for such a high LGM inventory of P is largely circumstantial, making it, in our opinion, an unlikely scenario.

[67] Provided the P inventory did not change across the deglacial transition, marine phytoplankton would have lived in a N-rich ocean, where PO_4^{3-} rather than NO_3^- would have been the proximate limiting nutrient [*Tyrrell*, 1999]. Alternatively, it would have required a plankton community with a higher average biomass N:P ratio [*Weber and Deutsch*, 2012]. In fact, PO_4^{3-} would have been the proximate and ultimate limiting nutrient in such a LGM ocean, similar to the situation in the subtropical gyre of the North Atlantic [*Gruber and Sarmiento*, 1997; *Wu et al.*, 2000]. If the relative N:P requirements for non-N-fixing phytoplankton were fixed, such an increase in the N inventory would have led to only a marginal change in the global primary and export production. Therefore, despite a much larger N inventory during the LGM, we refrain from postulating a very strong contribution of an enhanced biological pump to the drawdown of atmospheric CO_2.

[68] A second biogeochemical implication of our results concerns the magnitude of the various N cycle feedbacks. In the standard case as well as in all sensitivity cases, the negative feedback associated with N-fixation (γ) turns out to be much stronger than the feedbacks associated with water column denitrification (α) or benthic denitrification (β) (Table S1). This means that denitrification has a very low sensitivity to changes in the marine N:P ratio, while N-fixation has a high sensitivity. These asymmetric feedbacks imply that a substantial temporary decoupling between N-fixation and denitrification can only occur if N-fixation is externally perturbed. If denitrification was externally perturbed, N-fixation would respond quickly, causing only a small temporary decoupling, which would lead to only a small change in the marine N inventory. This asymmetry in coupling may arise from the differences in how these two processes interact with each other. In the case of N-fixation, the response can occur faster, as any low N:P anomaly generated by denitrification can provide the niche for N-fixers when this anomaly arrives at the surface. In contrast, an excess of N:P generated by N-fixation may increase production and export anywhere in the world's ocean, but only that part of the increased export that occurs in the proximity of an OMZ can enhance water column denitrification. In the case of benthic denitrification, only that part of the enhanced export that occurs in the proximity of continental margins will cause an enhancement of benthic denitrification.

6. Summary and Conclusions

[69] Our model diagnoses a rather dynamic marine N cycle with the global N inventory decreasing by 16 to 50% across the last glacial termination. This large decrease is required in order to simultaneously fit the observational constraints in the OMZ, the oxic Indo-Pacific, and the low-latitude Atlantic. Of particular importance is the effect of the N inventory on the magnitude of the dilution effect, which determines how strongly water column denitrification in the OMZ determines the $\delta^{15}N$ of NO_3^- in the global ocean.

[70] The inventory decrease is largely caused by a strong temporary reduction in the rate of N-fixation at the beginning of the deglaciation, driven by a strong response of this process to a decrease in iron-rich dust deposition. Although our results support the importance of iron in controlling N-fixation, they also refute the hypothesis of much higher N-fixation rates during the LGM, such as promoted by *Falkowski* [1997] and *Broecker and Henderson* [1998]. The global rate of water column denitrification increases by 10 to 100% across the transition compared to the glacial rate, while the change in the global rate of benthic denitrification ranges from –1 to 58%. Thus, compared to the "canonical description" of the deglacial N cycle, which emphasizes the role of the onset of water column denitrification as the most important driver of change, our model emphasizes the role of N-fixation as the first process to change and having the most important impact on the change in the marine N inventory.

[71] These results are robust with regard to nearly all of the parameters and assumptions used in the model, with the exception of the possibility of a major change in ocean circulation and in particular the ventilation of the OMZ. Indeed, the impact of such changes in ocean circulation and mixing is the most important caveat of our data-assimilation study. Although the data constraints on the glacial circulation are continuously increasing [*Curry and Oppo*, 2005; *Gherardi et al.*, 2009], we consider the knowledge of the most critical circulation aspects for this work, i.e., the ventilation of the thermocline and especially that of the anoxic regions in

the Pacific and Indian Ocean as too uncertain to incorporate it explicitly in our model. Clearly, as we learn more about the deglacial evolution of the ocean's circulation, it is imperative to revisit our assumption and to assess its full impact. Based on our initial sensitivity study, we expect a reduction in the magnitude of the glacial-to-interglacial N inventory, but it is rather likely that our finding of more complex evolution of N-fixation and denitrification across the last deglaciation is here to stay.

[72] Although we diagnose the LGM inventory of N to be substantially larger than that of the late Holocene, we argue that this likely did not lead to a large increase in primary and export production. Thus, these changes likely had only a limited contribution to the lower glacial atmospheric CO_2 levels. However, the N-rich ocean of the LGM made PO_4^{3-} the most important limiting nutrient, likely causing shifts in the phytoplankton communities.

[73] Our results reveal that great care is needed when interpreting $\delta^{15}N$ data from individual sites, as their temporal evolutions are typically as strongly governed by global processes as they are by basin-scale processes. Additional care is required when relating N cycle processes to the evolution of potential drivers, as the role of these drivers can change through time and because the processes can respond highly nonlinearly to the forcings. Proper attribution of drivers and feedbacks require the interpretation of these data with tools that explicitly consider the spatiotemporal dynamics of the marine N cycle.

[74] **Acknowledgments.** We would like to thank Diego Santaren for supplying the genetic algorithm and the many scientists and technicians who measured the $\delta^{15}N$ data and made them available. This work was supported by funds from ETH Zurich. We are very grateful to the three anonymous reviewers who provided us with precious advice and constructive comments. Their detailed and meticulous reviews were appreciated and greatly improved this submission.

References

Alkhatib, M., M. F. Lehmann, and P. A. del Giorgio (2012), The nitrogen isotope effect of benthic remineralization-nitrification-denitrification coupling in an estuarine environment, *Biogeosciences*, *9*(5), 1633–1646, doi:10.5194/bg-9-1633-2012.

Altabet, M. A. (2007), Constraints on oceanic N balance/imbalance from sedimentary ^{15}N records, *Biogeosciences*, *4*(1), 75–86, doi:10.5194/bg-4-75-2007.

Altabet, M. A., W. G. Deuser, S. Honjo, and C. Stienen (1991), Seasonal and depth-related changes in the source of sinking particles in the North Atlantic, *Nature*, *354*(6349), 136–139.

Altabet, M. A., R. Francois, D. W. Murray, and W. L. Prell (1995), Climate-related variations in denitrification in the Arabian Sea from sediment $^{15}N/^{14}N$ ratios, *Nature*, *373*(6514), 506–509.

Altabet, M. A., M. J. Higginson, and D. W. Murray (2002), The effect of millennial-scale changes in Arabian Sea denitrification on atmospheric CO_2, *Nature*, *415*(6868), 159–162, doi:10.1038/415159a.

Archer, D., A. Winguth, D. Lea, and N. Mahowald (2000), What caused the glacial/interglacial atmospheric pCO_2 cycles? *Rev. Geophys.*, *38*(2), 159–189.

Bard, E., B. Hamelin, R. G. Fairbanks, and A. Zindler (1990), Calibration of the ^{14}C timescale over the past 30,000 years using mass-spectrometric U-Th ages from Barbados corals, *Nature*, *345*(6274), 405–410.

Benitez-Nelson, C. R. (2000), The biogeochemical cycling of phosphorus in marine systems, *Earth-Science Rev.*, *51*(1-4), 109–135.

Bianchi, D., J. P. Dunne, J. L. Sarmiento, and E. D. Galbraith (2012), Data-based estimates of suboxia, denitrification, and N_2O production in the ocean and their sensitivities to dissolved O_2, *Global Biogeochem. Cycles*, *26*, GB2009, doi:10.1029/2011GB004209.

Brandes, J. A., and A. H. Devol (1997), Isotopic fractionation of oxygen and nitrogen in coastal marine sediments, *Geochim. Cosmochim. Acta*, *61*(9), 1793–1801.

Brandes, J. A., and A. H. Devol (2002), A global marine-fixed nitrogen isotopic budget: Implications for Holocene nitrogen cycling, *Global Biogeochem. Cycles*, *16*(4), 1120, doi: 10.1029/2001GB001856.

Brandes, J. A., A. H. Devol, T. Yoshinari, D. A. Jayakumar, and S. W. A. Naqvi (1998), Isotopic composition of nitrate in the central Arabian Sea and eastern tropical North Pacific: A tracer for mixing and nitrogen cycles, *Limnol. Oceanogr.*, *43*(7), 1680–1689.

Broecker, W. S., and G. M. Henderson (1998), The sequence of events surrounding Termination II and their implications for the cause of glacial-interglacial CO_2 changes, *Paleoceanography*, *13*(4), 352–364.

Capone, D. G., J. P. Zehr, H. W. Paerl, B. Bergman, and E. J. Carpenter (1997), *Trichodesmium*, a globally significant marine cyanobacterium, *Science*, *276*, 1221–1229.

Carpenter, E. J., H. R. Harvey, B. Fry, and D. G. Capone (1997), Biogeochemical tracers of the marine cyanobacterium *Trichodesmium*, *Deep Sea Res. I*, *44*(1), 27–38.

Cline, J. D., and I. R. Kaplan (1975), Isotopic fractionation of dissolved nitrate during denitrification in the Eastern Tropical North Pacific Ocean, *Mar. Chem.*, *3*, 271–299.

Codispoti, L. A. (1989), Phosphorus vs. nitrogen limitation of new and export production, in *Productivity of the Ocean: Present and Past*, edited by W. H. Berger, V. S. Smetacek, and G. Wefer, John Wiley and Sons, New York, 337–394.

Codispoti, L. A., J. A. Brandes, J. P. Christensen, A. H. Devol, S. W. A. Naqvi, H. W. Paerl, and T. Yoshinari (2001), The oceanic fixed nitrogen and nitrous oxide budgets: Moving targets as we enter the anthropocene? *Sci. Mar.*, *65*(Suppl. 2), 85–105.

Curry, W. B., and D. W. Oppo (2005), Glacial water mass geometry and the distribution of $\delta^{13}C$ of sigmaCO_2 in the western Atlantic Ocean, *Paleoceanography*, *20*(1), PA1017, doi:10.1029/2004PA001021.

De Pol-Holz, R., O. Ulloa, L. Dezileau, J. Kaiser, F. Lamy, and D. Hebbeln (2006), Melting of the Patagonian Ice Sheet and deglacial perturbations of the nitrogen cycle in the eastern South Pacific, *Geophys. Res. Lett.*, *33*(4), L04704, doi:10.1029/2005GL024477.

Delaney, M. L. (1998), Phosphorus accumulation in marine sediments and the oceanic phosphorus cycle, *Global Biogeochem. Cycles*, *12*(4), 563–572.

Deutsch, C., and T. Weber (2012), Nutrient ratios as a tracer and driver of ocean biogeochemistry, *Ann. Rev. Mar. Sci.*, *4*, 113–141, doi: 10.1146/annurev-marine-120709-142821.

Deutsch, C., D. M. Sigman, R. C. Thunell, A. N. Meckler, and G. H. Haug (2004), Isotopic constraints on glacial/interglacial changes in the oceanic nitrogen budget, *Global Biogeochem. Cycles*, *18*, GB4012, doi: 10.1029/2003GB002189.

Deutsch, C., J. L. Sarmiento, D. M. Sigman, N. Gruber, and J. P. Dunne (2007), Spatial coupling of nitrogen inputs and losses in the ocean, *Nature*, *445*, 163–167, doi:10.1038/nature05392.

DeVries, T., C. Deutsch, F. Primeau, B. Chang, and A. Devol (2012), Global rates of water-column denitrification derived from nitrogen gas measurements, *Nature Geosci.*, *5*(8), 547–550, doi: 10.1038/NGEO1515.

Duplessy, J. C., N. J. Shackleton, R. G. Fairbanks, L. Labeyrie, D. Oppo, and N. Kallel (1988), Deepwater source variations during the last climatic cycle and their impact on the global deepwater circulation, *Paleoceanography*, *3*(3), 343–360, doi:10.1029/PA003i003p00343.

Dutkiewicz, S., B. A. Ward, F. Monteiro, and M. J. Follows (2012), Interconnection of nitrogen fixers and iron in the Pacific Ocean: Theory and numerical simulations, *Global Biogeochem. Cycles*, *26*, GB1012, doi: 10.1029/2011GB004039.

Eugster, O., and N. Gruber (2012), A probabilistic estimate of global marine N-fixation and denitrification, *Global Biogeochem. Cycles*, *26*(40), GB4013, doi:10.1029/2012GB004300.

Falkowski, P. G. (1997), Evolution of the nitrogen cycle and its influence on the biological sequestration of CO_2 in the ocean, *Nature*, *387*, 272–275, doi:10.1038/387272a0.

Francois, R., M. A. Altabet, and L. H. Burckle (1992), Glacial to interglacial changes in surface nitrate utilization in the Indian Sector of the Southern Ocean as recorded by sediment $\delta^{15}N$, *Paleoceanography*, *7*(5)

Galbraith, E. D., M. Kienast, T. F. Pedersen, and S. E. Calvert (2004), Glacial-interglacial modulation of the marine nitrogen cycle by oxygen supply to intermediate waters, *Paleoceanography*, *19*, PA4007, doi: 10.1029/2003PA001000.

Ganeshram, R. S., T. F. Pedersen, S. E. Calvert, and R. Francois (2002), Reduced nitrogen fixation in the glacial ocean inferred from changes in marine nitrogen and phosphorus inventories, *Nature*, *415*, 156–159, doi: 10.1038/415156a.

Gherardi, J.-M., L. Labeyrie, S. Nave, R. Francois, J. F. McManus, and E Cortijo (2009), Glacial-interglacial circulation changes inferred from $^{231}Pa/^{230}Th$ sedimentary record in the North Atlantic region, *Paleoceanography*, *24*, PA2204, doi:10.1029/2008PA001696.

Granger, J., M. G. Prokopenko, D. M. Sigman, C. W. Mordy, Z. M. Morse, L. V. Morales, R. N. Sambrotto, and B. Plessen (2011), Coupled nitrification-denitrification in sediment of the eastern Bering Sea shelf leads to ^{15}N enrichment of fixed N in shelf waters, *J. Geophysical Research-Oceans*, *116*, C11006, doi:10.1029/2010JC006751.

Gruber, N. (2004), The dynamics of the marine nitrogen cycle and atmospheric CO_2, in *Carbon Climate Interactions*, edited by T. Oguz, and M. Follows, Kluwer Academic, Dordrecht, 97–148.

Gruber, N., and J. L. Sarmiento (1997), Global patterns of marine nitrogen fixation and denitrification, *Global Biogeochem. Cycles*, *11*(2), 235–266, doi:10.1029/97GB00077.

Hamersley, M. R., K. A. Turk, A. Leinweber, N. Gruber, J. P. Zehr, T. Gunderson, and D. G. Capone (2011), Nitrogen fixation within the water column associated with two hypoxic basins in the Southern California Bight, *Aquat. Microb. Ecol.*, *63*(2), 923–933.

Hanebuth, T., K. Stattegger, and P. M. Grootes (2000), Rapid flooding of the Sunda Shelf: A late-glacial sea-level record, *Science*, *288*(5468), 1033–1035.

Haug, G. H., T. F. Pedersen, D. M. Sigman, S. E. Calvert, B. Nielsen, and L. C. Peterson (1998), Glacial/interglacial variations in production and nitrogen fixation in the Cariaco Basin during the last 580 kyr, *Paleoceanography*, *13*(5), 427–432.

Hutchins, D. A., F. X. Fu, Y. Zhang, M. E. Warner, Y. Feng, K. Portune, P. W. Bernhardt, and M. R. Mulholland (2007), CO_2 control of *Trichodesmium* N_2 fixation, photosynthesis, growth rates, and elemental ratios: Implications for past, present, and future ocean biogeochemistry, *Limnol. Oceanogr.*, *52*(4), 1293–1304, doi:10.4319/lo.2007.52.4.1293.

Ivanochko, T. S., R. S. Ganeshram, G. J. A. Brummer, G. Ganssen, S. J. A. Jung, S. G. Moreton, and D. Kroon (2005), Variations in tropical convection as an amplifier of global climate change at the millennial scale, *Earth Planetary Science Lett.*, *235*(1-2), 302–314, doi: 10.1016/j.epsl.2005.04.002.

Jaccard, S. L., and E. D. Galbraith (2012), Large climate-driven changes of oceanic oxygen concentrations during the last deglaciation, *Nature Geosci.*, *5*(2), 151–156, doi:10.1038/NGEO1352.

Karl, D. M., A. F. Michaels, B. Bergman, D. Capone, E. Carpenter, R. Letelier, F. Lipschultz, H. Paerl, D. Sigman, and L. Stal (2002), Dinitrogen fixation in the World's oceans, *Biogeochemistry*, *57* (1), 47–98, doi: 10.1023/A:1015798105851.

Keigwin, L. D., and G. A. Jones (1990), Deglacial climatic oscillations in the gulf of California, *Paleoceanography*, *5*(6), 1009–1023.

Kienast, M. (2000), Unchanged nitrogen isotopic composition of organic matter in the South China Sea during the last climatic cycle: Global implications, *Paleoceanography*, *15*(2), 244–253.

Kohfeld, K. E., C. L. Quere, S. P. Harrison, and R. F. Anderson (2005), Role of marine biology in glacial-interglacial CO_2 cycles, *Science*, *308*(5718), 74–78, doi:10.1126/science.1105375.

Lehmann, M. F., D. M. Sigman, D. C. McCorkle, J. Granger, S. Hoffmann, G. Cane, and B. G. Brunelle (2007), The distribution of nitrate $^{15}N/^{14}N$ in marine sediments and the impact of benthic nitrogen loss on the isotopic composition of oceanic nitrate, *Geochim. Cosmochim. Acta*, *71*(22), 5384–5404, doi:10.1016/j.gca.2007.07.025.

Lynch-Stieglitz, J., et al. (2007), Atlantic meridional overturning circulation during the Last Glacial Maximum, *Science*, *316*(5821), 66–69, doi: 10.1126/science.1137127.

McElroy, M. B. (1983), Marine biological controls on atmospheric CO_2 and climate, *Nature*, *302*, 328–329, doi: 10.1038/302328a0.

Meckler, A. N., H. J. Ren, D. M. Sigman, N. Gruber, B. Plessen, C. J. Schubert, and G. H. Haug (2011), Deglacial nitrogen isotope changes in the Gulf of Mexico: Evidence from bulk sedimentary and foraminifera-bound nitrogen in Orca Basin sediments, *Paleoceanography*, *26*, PA4216, doi: 10.1029/2011PA002156.

Middelburg, J. J., K. Soetaert, P. M. J. Herman, and C. H. R. Heip (1996), Denitrification in marine sediments: A model study, *Global Biogeochem. Cycles*, *10*(4), 661–673, doi: 10.1029/96GB02562.

Monteiro, F. M., S. Dutkiewicz, and M. J. Follows (2011), Biogeographical controls on the marine nitrogen fixers, *Global Biogeochem. Cycles*, *25*, GB2003, doi:10.1029/2010GB003902.

Paerl, H. W., L. E. Prufertbebout, and C. Z. Guo (1994), Iron-stimulated N_2 fixation and growth in natural and cultured populations of the planktonic marine cyanobacteria, *Trichodesmium spp Appl. Environ. Microbiol.*, *60*(3), 1044–1047.

Petit, J. R., et al. (1999), Climate and atmospheric history of the past 420,000 years from Vostok ice core, Antarctica, *Nature*, *399*, 429–436.

Ren, H., D. M. Sigman, A. N. Meckler, B. Plessen, R. S. Robinson, Y. Rosenthal, and G. H. Haug (2009), Foraminiferal isotope evidence of reduced nitrogen fixation in the ice age Atlantic Ocean, *Science*, *323*(5911), 244–248, doi:10.1126/science.1165787.

Ren, H., D. M. Sigman, M.-T. Chen, and S.-J. Kao (2012), Elevated foraminifera-bound nitrogen isotopic composition during the last ice age in the South China Sea and its global and regional implications, *Global Biogeochem. Cycles*, *26*, GB1031, doi:10.1029/2010GB004020.

Schmittner, A., and E. D. Galbraith (2008), Glacial greenhouse-gas fluctuations controlled by ocean circulation changes, *Nature*, *456*, 373–376, doi:10.1038/nature07531.

Sigman, D. M., M. A. Altabet, D. D. McCorkle, R. Francois, and G. Fischer (1999), The $\delta^{15}N$ of nitrate in the Southern Ocean: Consumption of nitrate in surface waters, *Global Biogeochem. Cycles*, *13*(4), 1149–1166, doi:10.1029/1999GB900038.

Somes, C. J., A. Schmittner, E. D. Galbraith, M. F. Lehmann, M. A. Altabet, J. P. Montoya, R. M. Letelier, A. C. Mix, A. Bourbonnais, and M. Eby (2010), Simulating the global distribution of nitrogen isotopes in the ocean, *Global Biogeochem. Cycles*, *24*, GB4019, doi: 10.1029/2009GB003767.

Tamburini, F., and K. B. Foellmi (2009), Phosphorus burial in the ocean over glacial-interglacial time scales, *Biogeosciences*, *6* (4), 501–513, doi:10.5194/bg-6-501-2009.

Thunell, R. C., D. M. Sigman, F. Muller-Karger, Y. Astor, and R. Varela (2004), Nitrogen isotope dynamics of the Cariaco Basin, Venezuela, *Global Biogeochem. Cycles*, *18* (3), GB1001, doi: 10.1029/2002GB002028.

Tyrrell, T. (1999), The relative influences of nitrogen and phosphorus on oceanic primary production, *Nature*, *400*, 525–531.

Wallmann, K. (2010), Phosphorus imbalance in the global ocean? *Global Biogeochem. Cycles*, *24*, GB4030, doi:10.1029/2009GB003643.

Weber, T., and C. Deutsch (2012), Oceanic nitrogen reservoir regulated by plankton diversity and ocean circulation, *Nature*, *489* (7416), 419–422, doi:10.1038/nature11357.

Weber, T. S., and C. Deutsch (2010), Ocean nutrient ratios governed by plankton biogeography, *Nature*, *467* (7315), 550–554, doi: 10.1038/nature09403.

Wong, G. T. F., C.-M. Tseng, L.-S. Wen, and S.-W. Chung (2007), Nutrient dynamics and N-anomaly at the SEATS station, *Deep Sea Res. II*, *54*(14-15), 1528–1545, doi:10.1016/j.dsr2.2007.05.011.

Wu, J. F., W. Sunda, E. A. Boyle, and D. M. Karl (2000), Phosphate depletion in the western North Atlantic Ocean, *Science*, *289*(5480), 759–762.

Yung, Y. L., T. Lee, C.-H. Wang, and Y.-T. Shieh (1996), Dust: A diagnostic of the hydrologic cycle during the last glacial maximum, *Science*, *271*, 962–963.